

# Enzymeless voltammetric hydrogen peroxide sensor based on the use of PEDOT doped with Prussian Blue nanoparticles

Junjie Wang<sup>1</sup> · Yu Wang<sup>1</sup> · Min Cui<sup>1</sup> · Shenghao Xu<sup>1</sup> · Xiliang Luo<sup>1</sup>

Received: 29 July 2016 / Accepted: 19 November 2016 / Published online: 5 December 2016  
© Springer-Verlag Wien 2016

**Abstract** An electrochemical sensor for H<sub>2</sub>O<sub>2</sub> was developed based on electrochemically deposited Prussian blue (PB) nanoparticles doped poly(3,4-ethylenedioxythiophene) (PEDOT). The PEDOT/PB composite was composed of PEDOT wrapped PB nanoparticles, where the conducting polymer PEDOT not only protected the PB particles to warrant high stability, but also connected them to enhance the electron transfer. Owing to the excellent conductivity of PEDOT and unique electrocatalytic activity of PB, the PEDOT/PB modified electrode exhibited good catalytic activity toward the electrochemical reduction of H<sub>2</sub>O<sub>2</sub>, and was used for the detection of H<sub>2</sub>O<sub>2</sub> in concentrations ranging from 0.5 to 839 μM, with a detection limit of 0.16 μM. Moreover, the sensor also demonstrated excellent reproducibility, selectivity and long-term stability, showing great promise for the fabrication of electrochemical sensors and H<sub>2</sub>O<sub>2</sub> related biosensors.

**Keywords** Electroanalysis · Chemical sensor · Electrochemical deposition · Cyclic voltammetry · Conducting polymer · Nanocomposite

**Electronic supplementary material** The online version of this article (doi:10.1007/s00604-016-2025-y) contains supplementary material, which is available to authorized users.

✉ Xiliang Luo  
xiliangluo@qust.edu.cn

<sup>1</sup> Key Laboratory of Sensor Analysis of Tumor Marker, Ministry of Education, College of Chemistry and Molecular Engineering, Qingdao University of Science and Technology, Qingdao 266042, China

## Introduction

Many previous works have focused on the development of enzyme-based H<sub>2</sub>O<sub>2</sub> sensors, which may be restricted in practical application owing to the limited lifetimes, high costs, low stability and denaturation of enzymes. An effective way to overcome these disadvantages is to develop non-enzymatic sensors for H<sub>2</sub>O<sub>2</sub> detection. Various materials have been used for the fabrication of sensors, including metal [1–6], polypyrrole [7], MoS<sub>2</sub> [8], carbon nanotubes [9] and materials with enzyme-like activities, such as Prussian blue (PB) [10].

PB, an “artificial enzyme peroxidase”, has been widely used as an electron transfer mediator for the construction of oxidase-based electrochemical biosensors due to its excellent reversible redox properties and good catalytic property [11–13]. However, the immobilization of electron-shuttling mediators on the interfaces of electrode faces several challenges, which is particularly true for soluble mediators with low molecular weight, because they can easily diffuse away from the electrode surface into the surrounding solution, leading to poor response performance. Nanoparticles, with increased size and molecular weights, can well address this problem owing to their unique chemical and physical properties [14, 15]. As a result of their extended surfaces, the improved activities of nanoparticles make them promising candidates for sensing and catalysis. Up to now, the synthesis and properties of PB nanoparticles have been well established [16, 17]. PB nanoparticles with improved stability have been widely used in the electrochemical sensor field due to their large surface-to-volume ratio and enhanced electrochemical properties [18, 19]. However, it is still a challenge for researchers to find suitable strategies for PB immobilization, without sacrificing its activity.

Conducting polymers have also been extensively used in the development of sensors because of their good electrical,

optical and electrocatalytic properties [20]. Among various conducting polymers, poly(3, 4-ethylenedioxythiophene) (PEDOT) has been considered as the most promising one due to its outstanding stability and conductivity [21, 22]. Kulesza' group has fabricated a structured film composed of a layer of compact chemically formed PB and a layer of electrodeposited PEDOT (the PB based inner layer was covered by PEDOT) to develop an enzyme-based biosensor for H<sub>2</sub>O<sub>2</sub> detection [23]. In this work, pre-synthesized PB nanoparticles were electrodeposited together with PEDOT onto an electrode surface to form a homogeneous nanocomposite of PEDOT/PB in a single step. The prepared PEDOT/PB nanocomposite, with PB nanoparticles protected by a thin layer of highly conductive PEDOT, possessed a grape-like microstructure with a large surface area. The deposited PEDOT/PB exhibited excellent stability and catalytic activity, and it was directly used for the development of a non-enzymatic electrochemical H<sub>2</sub>O<sub>2</sub> sensor.

## Experimental

### Reagents

3,4-ethylenedioxythiophene (EDOT), ascorbic acid (AA), uric acid (UA), and dopamine (DA) were purchased from Aladdin Ltd. (Shanghai, China) (<http://www.aladdin-e.com/>). Acetone was purchased from Yantai Sanhe Chemical Reagent Co., China (<http://11365509.czvv.com/>). All reagents were of analytical grade and used as received. Millipore water from a Milli-Q water purifying system was used throughout all experiments.

### Apparatus

Electrochemical experiments were carried out with the CHI760D electrochemical workstation (CH Instruments, Shanghai, China) (<http://www.chinstr.com/>), using a conventional three-electrode system with the platinum wire as the counter electrode, Ag/AgCl (3 M KCl) as the reference electrode and the glassy carbon electrode (GCE, diameter 3.0 mm) or modified GCE as the working electrode. The surface morphologies and microstructures of the modified electrodes were examined using a field emission scanning electron microscopy (SEM) instrument (JSM-7500F, Hitachi High-Technology Co., Japan), with an acceleration voltage of 5.0 kV. X-Ray photoelectron spectroscopy (XPS) analysis was conducted using an AXIS Ultra spectrometer with a high-performance Al monochromatic source operated at 15 kV. Transmission electron microscopy (TEM) was performed at a JEOL2010F transmission electron microscope at 20 kV.

### Synthesis of PB nanoparticles

PB nanoparticles were synthesized via a facile one-step method according to the previous report [24]. 100 mL of 1.0 mM K<sub>3</sub>[Fe(CN)<sub>6</sub>] was added dropwise into an aqueous solution of 1.0 mM FeCl<sub>2</sub> solution (100 mL) under vigorous stirring condition. The color of the solution gradually changed to dark blue, indicating that PB nanoparticles were formed. Then 400 mL of acetone was added into the above-mentioned reaction mixture to precipitate the nanoparticles. The resultant precipitate was separated by centrifugation at 9000 rpm (with a centrifugational force of 12,829 g) for 30 min and further cleaned using acetone repeatedly for three times.

### Fabrication of PB doped PEDOT modified electrodes

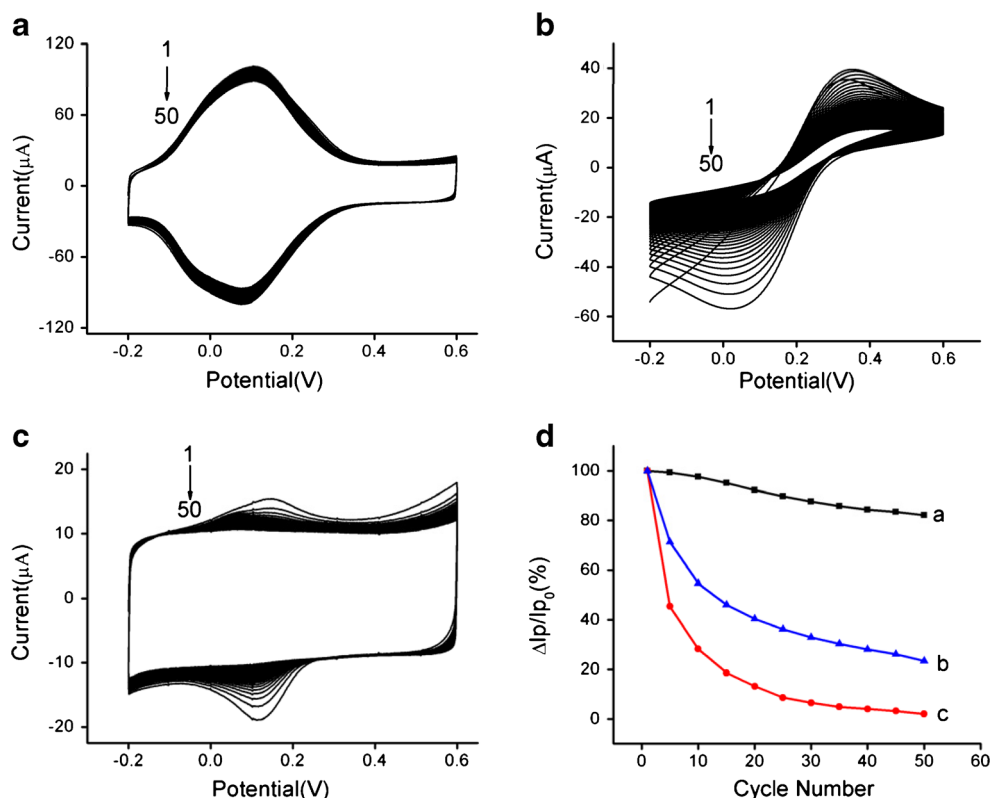
PEDOT/PB nanocomposite films were electrochemically deposited onto GCE surfaces from a solution of 2.0 mL water containing 2.0 mg mL<sup>-1</sup> PB nanoparticles and 0.02 M EDOT, using a constant potential of 1.0 V for 50 s. GCEs modified with the PEDOT/PB nanocomposite were denoted as PEDOT/PB/GCE. For comparison, GCE modified with PEDOT polymerized in a solution containing 2.0 mg mL<sup>-1</sup> K<sub>3</sub>[Fe(CN)<sub>6</sub>] and 0.02 M EDOT was prepared similarly (denoted as PEDOT/K<sub>3</sub>[Fe(CN)<sub>6</sub>]/GCE); PB nanoparticles modified GCE was prepared by drop-coating 2.0 mg mL<sup>-1</sup> PB nanoparticles solution (10 μL) onto the electrode surface and dried in air (denoted as PB/GCE). Cyclic voltammograms (CVs) were recorded at a scan rate of 100 mV s<sup>-1</sup>. For the electrochemical detection of H<sub>2</sub>O<sub>2</sub>, different concentrations of H<sub>2</sub>O<sub>2</sub> were added to the stirring N<sub>2</sub>-saturated phosphate buffered saline (PBS, 0.2 M, containing 0.9% NaCl) and the generated current was recorded using amperometric i-t curve technique with an applied potential of 0.0 V.

## Results and discussion

### Choice of materials

PEDOT has been considered to be one of the most promising conducting polymers due to its outstanding stability and conductivity. PB nanoparticles have been widely used owing to its excellent reversible redox properties and good catalytic property. However, the electrochemical stability of PB is unsatisfactory in many cases. Herein, PB nanoparticles were coated with electrodeposited PEDOT through a simple electropolymerization process, in order to improve the stability of PB and at the same time keep its electrochemical activity. The stability of the PEDOT/PB/GCE was tested in PBS (0.2 M, pH 5.7) using CV between -0.2 V and 0.6 V for 50 cycles (Fig. 1a). The PEDOT/PB/GCE shows excellent

**Fig. 1** **a** CVs of PEDOT/PB/GCE, **b** PB/GCE and **c** PEDOT/ $K_3[Fe(CN)_6]$ /GCE in 0.2 M PBS (pH 5.7), scan rate:  $100\text{ mV s}^{-1}$ . **d** Reduction peak current changes of (a) the PEDOT/PB/GCE, (b) the PB/GCE and (c) the PEDOT/ $K_3[Fe(CN)_6]$ /GCE at different cycle numbers



stability with slight decrease in currents of the redox peaks even after 50 CV cycles. For comparison, PEDOT/ $K_3[Fe(CN)_6]$ /GCE (Fig. 1c) and PB/GCE (Fig. 1b) were fabricated, respectively, and tested their stabilities under the same condition. In sharp contrast, significant decrease in currents was observed for the redox peaks of both the PEDOT/ $K_3[Fe(CN)_6]$ /GCE and the PB/GCE after 50 cycles. The peak current of the PB/GCE decreased significantly and it retained only 23.3% of its initial peak current after 50 cycles (Fig. 1d). The PEDOT/PB modified electrode was able to retain 82.3% of its initial value after 50 cycles, while the PEDOT/ $K_3[Fe(CN)_6]$  just retained 2.0%. This result clearly shows improved stability of the PEDOT/PB nanocomposite, verifying effective protection of PB with the conducting polymer PEDOT.

#### Characterization of PB nanoparticles and the PB doped PEDOT nanocomposite

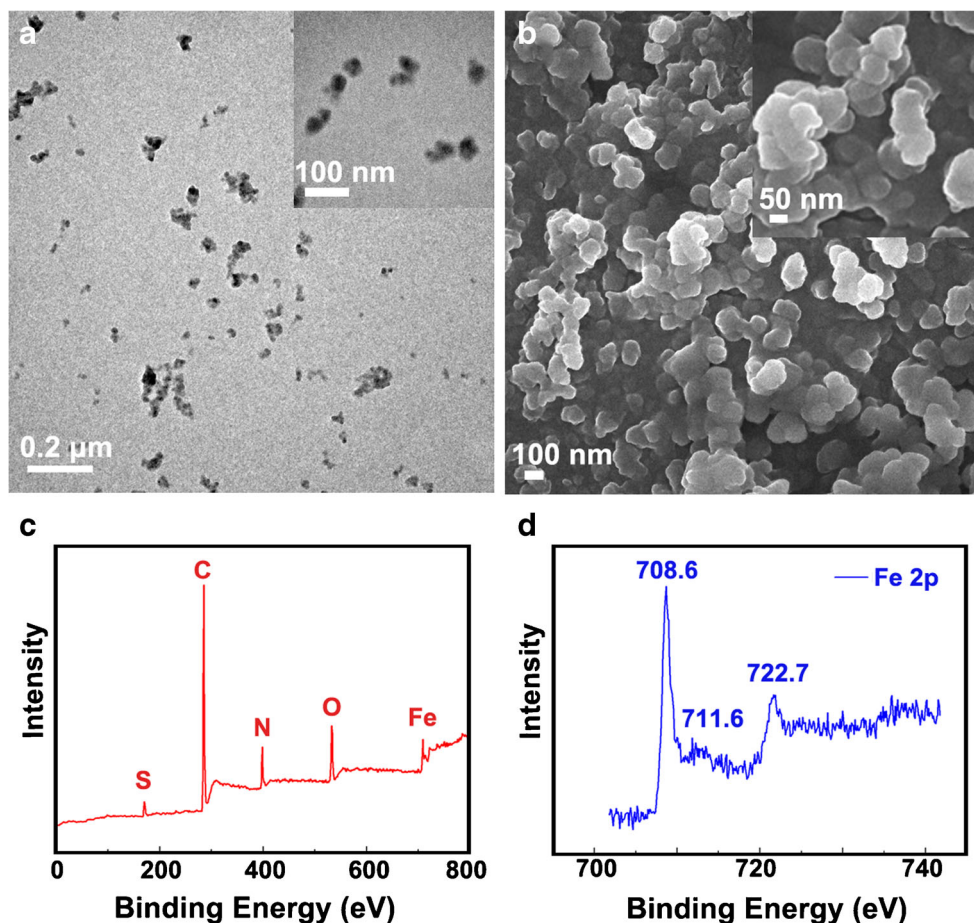
TEM images of the PB nanoparticles are shown in Fig. 2a. The PB nanoparticles are well-dispersed and show an average diameter of approximately 40 nm. Figure 2b shows the SEM images of the PEDOT/PB nanocomposite/GCE. The PEDOT/PB film shows a grape-like microstructure, possessing a porous structure in the nanoscale with an enlarged surface area. The diameter of the PEDOT/PB particles was about 60–100 nm, which is significantly larger than that of the PB

nanoparticles. As PB nanoparticles were the only dopant for the electrochemical polymerization of PEDOT, this unique grape-like microstructure might be formed through the wrapping of PB by a thin layer of PEDOT. That was, the PEDOT was polymerized around the PB nanoparticles, which connect different PB nanoparticles and protect the PB nanoparticles as a covering shell.

As shown in Fig. 2c, C 1 s, N 1 s, O 1 s, S 2p and Fe 2p core-level photoemission spectra all appeared on the XPS spectrum. Judging from the Fe 2p pattern of the PEDOT/PB nanocomposite shown in Fig. 2d, it can be revealed that the levels of Fe  $2p_{3/2}$  and Fe  $2p_{1/2}$  located at 711.6 eV and 722.7 eV, respectively, which came from the  $Fe^{3+}$  of PB nanoparticles. Moreover, an additional XPS peak at 708.6 eV can be attributed to the Fe  $2p_{3/2}$  of  $[Fe(CN)_6]^{4-}$ , which was consistent with the previous literature [25].

Figure 3 shows the electrochemical impedance spectroscopy (EIS) Nyquist plots of different electrodes recorded in 5.0 mM  $[Fe(CN)_6]^{4-3-}$  solution containing 0.1 M KCl. The semicircle portion of the plot corresponds to the charge transfer process, with the diameter of the semicircle equivalent to the charge transfer resistance ( $R_{ct}$ ) [26], while the linear portion reflects the diffusion limited process at the electrode interface. Clearly, with the electrochemical deposition of PEDOT/PB on the GCE, the PEDOT/PB/GCE (curve a) shows a much lower  $R_{ct}$  than that of the bare GCE (curve b). This result may be ascribed to the fact that the

**Fig. 2** **a** TEM images of PB nanoparticles, **b** SEM images of the PEDOT/PB Nanocomposite, **c** XPS full survey spectrum of the as-prepared PEDOT/PB nanocomposite, **d** Fe 2p XPS spectrum of the PEDOT/PB nanocomposite



electrodeposited nanocomposite film is conductive and provides an increased effective surface on the electrode.

### Electrochemical response to hydrogen peroxide

The electrochemical behavior of the PEDOT/PB/GCE was investigated by cyclic voltammograms. As shown in Fig. 4 curve a1, the PEDOT/PB/GCE exhibited a pair of well-defined redox peaks, corresponding to the reversible

conversion of PB to Prussian white [18, 27]. In the presence of  $\text{H}_2\text{O}_2$ , the cathodic peak current of the PEDOT/PB/GCE is increased and the anodic peak current decreased (curve a2), indicating excellent catalytic property of the PEDOT/PB to the reduction of  $\text{H}_2\text{O}_2$ . However, for the bare GCE and the GCE modified with PEDOT doped with an inert macromolecule, poly(sodium-p-styrenesulfonate) (PSS), they show no obvious redox peaks in PBS (Fig. 4, curves c1 and b1), owing to the lack of redox probe like PB. After the addition of  $\text{H}_2\text{O}_2$ ,

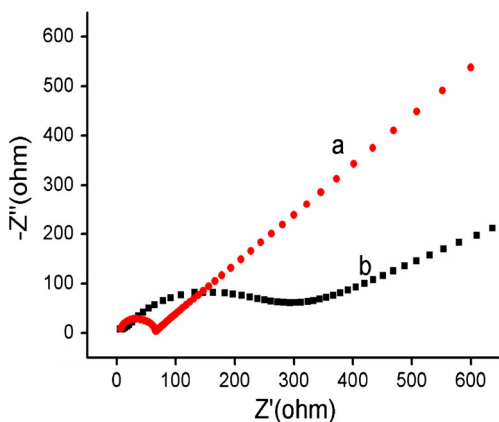


**Fig. 3** Nyquist plots of the EIS for the PEDOT/PB/GCE **a** and the bare GCE **b** in 5.0 mM  $[\text{Fe}(\text{CN})_6^{4-/3-}]$  solution containing 0.1 M KCl

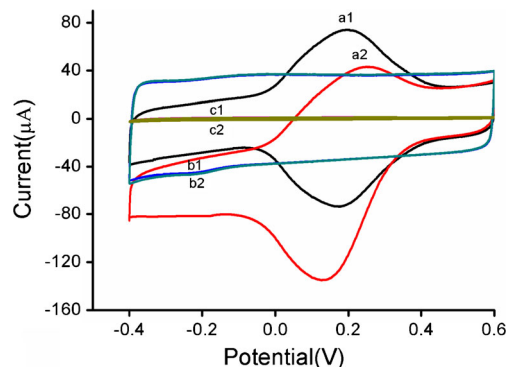
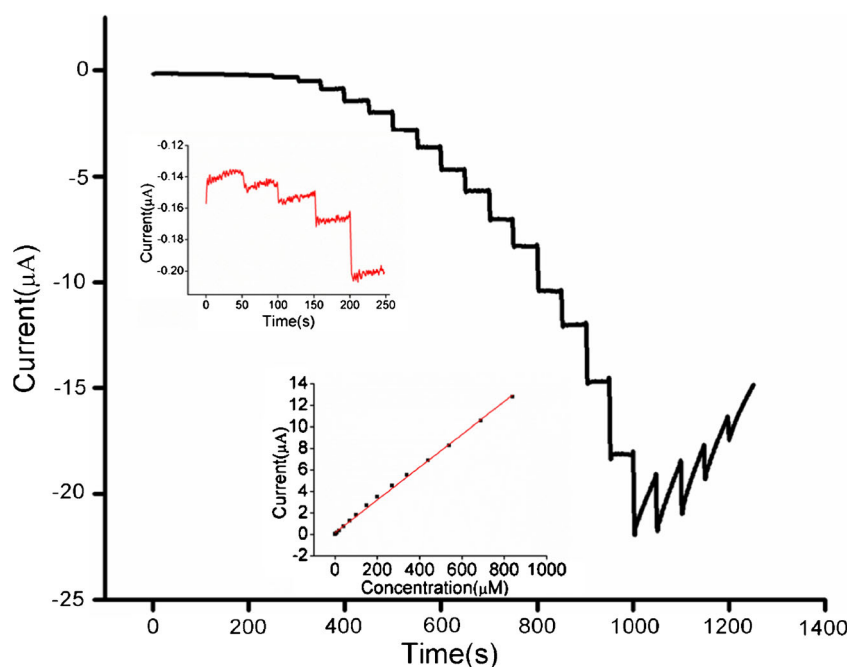


**Fig. 4** CVs of the PEDOT/PB/GCE (curves a1 and a2), PEDOT/PSS/GCE (curves b1 and b2) and bare GCE (curves c1 and c2) in 0.2 M PBS (pH 5.7) in the absence (curves a1, b1 and c1) and presence (curves a2, b2 and c2) of 4.0 mM  $\text{H}_2\text{O}_2$ , scan rate:  $100 \text{ mV s}^{-1}$



**Fig. 5** Amperometric responses of PEDOT/PB/GCE toward the successive additions of  $\text{H}_2\text{O}_2$  into stirring 0.2 M PBS (pH 4.0). The working potential was 0.0 V, and the  $\text{H}_2\text{O}_2$  concentrations added were 0.5, 0.8, 1.0, 2.0, 5.0, 10.0, 20.0, 30.0, 30.0, 50.0, 50.0, 70.0, 70.0, 100.0, 100.0 and 150.0  $\mu\text{M}$  in sequence, and the rest additions were all 150.0  $\mu\text{M}$ . Inset left, magnified portion of the amperometric response curve of the sensor. Inset right, the linear calibration curve of the  $\text{H}_2\text{O}_2$  sensor



there was no response for the GCE and the PEDOT/PSS/GCE (curves c2 and b2). Therefore, it can be concluded that the PEDOT/PB/GCE had high catalytic activity toward the reduction of  $\text{H}_2\text{O}_2$ , which might be ascribed to the effective incorporation of PB nanoparticles in the conductive PEDOT film.

### Detection of hydrogen peroxide

In order to optimize conditions for the detection of  $\text{H}_2\text{O}_2$ , the influence of the deposition time of the PEDOT/PB nanocomposite and the effect of pH of the electrolyte were investigated (Fig. S1 and S2, Supporting Information). It was found that the PEDOT/PB/GCE exhibited the maximum response when the deposition time was 50 s and the pH was 4.0, respectively. The effect of the applied potential on the sensor response was also studied with different potentials ranging from  $-0.1$  to  $0.3$  V (Fig. S3, Supporting Information). Clearly, the response current increased with an increase in the potential from  $-0.1$  V to  $0.0$  V and then decreased in the potential from  $0.0$  V to  $0.3$  V. Therefore, a deposition time of 50 s, a pH of 4.0 and

an applied potential of  $0.0$  V were selected as the optimum condition for the following measurements.

Figure 5 shows the amperometric *i-t* curve of the PEDOT/PB/GCE with successive addition of varying concentrations of  $\text{H}_2\text{O}_2$ . It can be observed that the PEDOT/PB/GCE exhibited a quick response to the injection of  $\text{H}_2\text{O}_2$ , and the steady-state current can be achieved within 5 s. Moreover, the calibration curve reveals a linear range of  $0.5$ – $839$   $\mu\text{M}$  ( $R^2 = 0.9981$ ). The limit of detection (LOD) of the  $\text{H}_2\text{O}_2$  sensor was calculated to be  $0.16$   $\mu\text{M}$  ( $S/N = 3$ ). Compared with other PB modified electrodes for  $\text{H}_2\text{O}_2$  [28–32] (Table 1), the PEDOT/PB/GCE sensor shows satisfying sensitivity and lower operation potential. The good sensitivity might be ascribed to the unique property of the PEDOT/PB nanocomposite. Firstly, the PEDOT/PB possessed a grape-like microstructure with large surface area for easy diffusion of  $\text{H}_2\text{O}_2$  molecules. Secondly, PB nanoparticles in the nanocomposite retained good catalytic activity as an artificial enzyme for  $\text{H}_2\text{O}_2$ . Finally, the highly conductive PEDOT bridged PB nanoparticles effectively accelerate the electron transfer. In addition, the operation potential

**Table 1** Comparison of different modified electrodes for  $\text{H}_2\text{O}_2$  determination

Electrode material	Linear range ( $\mu\text{M}$ )	Detection limit ( $\mu\text{M}$ )	Detection potential (V)	Reference
GO/PB	5–1200	0.122	0.1	[28]
PB	1–10, 10–100	0.36	-0.05	[29]
Au/MPS/PB	2–200	1.8	-0.2	[30]
GO-PB-Chit	1–1000	0.1	0.1	[31]
PB	50–6000	1	-0.1	[32]
PEDOT/PB	0.5–839	0.16	0.0	this work

of 0.0 V allowed the sensor to be able to free from interferences of many electroactive molecules.

A highly selective response to the analyte over potentially competing species is another requirement for an application in real sample test. The selectivity of the PEDOT/PB/GCE to  $\text{H}_2\text{O}_2$  over potentially interfering substances such as DA, AA, and UA was shown in Fig. 6. The sensor shows a clear response toward the addition of  $\text{H}_2\text{O}_2$ , while the successive addition of DA, AA and UA with a much higher concentration gives no significant response. The effects of lactose, Mg and Ca ions have also been tested, and they generated no electrochemical response at the applied low potential of 0.0 V. The above results indicate excellent selectivity of the sensor toward  $\text{H}_2\text{O}_2$ .

The reproducibility of the prepared  $\text{H}_2\text{O}_2$  sensor was also investigated. Five PEDOT/PB modified electrodes prepared independently were used to detect 10  $\mu\text{M}$   $\text{H}_2\text{O}_2$ , and the relative standard deviation (RSD) of these sensor responses was 4.5%, indicating excellent reproducibility. The stability of the sensor was also tested by measuring its current response to  $\text{H}_2\text{O}_2$  every a few days over a month. The sensor current response decreased by about 2.8% after the first week and 9.2% after 30 days when stored at room temperature. The satisfying reproducibility and stability, in addition to the excellent sensitivity and selectivity, makes the PEDOT/PB based sensor highly attractive for practical applications.

Small quantities of hydrogen peroxide were added to milk in order to prevent its spoilage or extend its longevity. This strategy was effective to control the microbial growth that leads to milk spoilage [33]. To investigate the feasibility of the fabricated  $\text{H}_2\text{O}_2$  sensor in practical application, the standard addition method was carried out to detect  $\text{H}_2\text{O}_2$  in milk. Milk samples were firstly diluted 100 times with 0.2 M PBS (pH 5.7) contains 0.9% (0.15 M) NaCl. Then 10 mL of the diluted milk samples was added into a small electrochemical cell and standard concentration of  $\text{H}_2\text{O}_2$  was spiked into the samples. As shown in Table 2, the recoveries ranged from

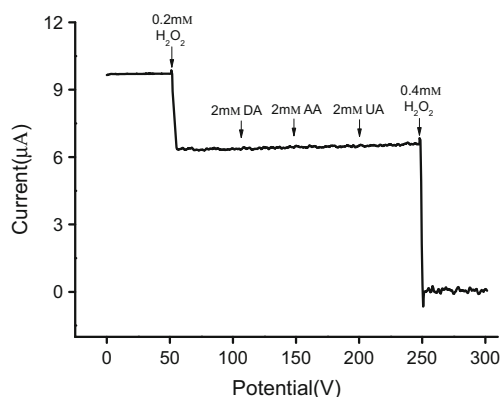


**Fig. 6** Amperometric response of the sensor toward  $\text{H}_2\text{O}_2$  and dopamine (DA), ascorbic acid (AA), and uric acid (UA) in 0.2 M PBS (pH 4.0). The applied potential is 0.0 V

**Table 2** Determination results of  $\text{H}_2\text{O}_2$  in milk samples ( $n = 5$ )

Sample	Added ( $\mu\text{M}$ )	Found ( $\mu\text{M}$ )	Recovery (%)	RSD (%)
1	5.0	5.1	102.0	3.8
2	10.0	9.8	98.0	2.4
3	15.0	15.4	102.7	3.3

98.0% to 102.7%, and the RSD was between 2.4–3.8%, indicating acceptable sensing performance.

## Conclusions

A  $\text{H}_2\text{O}_2$  electrochemical sensor was fabricated based on the electrodeposited conducting polymer PEDOT doped with PB nanoparticles. Owing to the protection and connection with highly conductive PEDOT, PB nanoparticles were very stable. The PEDOT/PB based sensor, with an interface suitable for  $\text{H}_2\text{O}_2$  diffusion and a conductive substrate favorable for electron transfer, exhibited a good sensitivity. The operation potential of 0.0 V for this electrochemical sensor warrants excellent selectivity even in the presence of other electroactive molecules. Considering its simple preparation method, excellent stability and electrochemical catalytic activity, the PEDOT/PB nanocomposite may become a promising material for constructing electrochemical sensors and biosensors associated with the assay of hydrogen peroxide. To further simplify the sensor fabrication, efforts may be made to obtain PEDOT/PB nanocomposite in one step without the pre-synthesis of PB nanoparticles.

**Acknowledgements** This research is supported by the National Natural Science Foundation of China (21275087, 21422504), the Natural Science Foundation of Shandong Province of China (JQ201406), and the Taishan Scholar Program of Shandong Province of China.

**Compliance with ethical standards** The author(s) declare that they have no competing interests.

## References

- Li Y, Zheng J, Sheng Q, Wang B (2015) Synthesis of Ag@AgCl nanoboxes, and their application to electrochemical sensing of hydrogen peroxide at very low potential. *Microchim Acta* 182(1–2): 61–68
- Yang Y, Fu R, Yuan J, Wu S, Zhang J, Wang H (2015) Highly sensitive hydrogen peroxide sensor based on a glassy carbon electrode modified with platinum nanoparticles on carbon nanofiber heterostructures. *Microchim Acta* 182(13–14):2241–2249
- Ming L, Peng T, Tu Y (2016) Multiple enhancement of luminol electrochemiluminescence using electrodes functionalized with titania nanotubes and platinum black: ultrasensitive determination of hydrogen peroxide, resveratrol, and dopamine. *Microchim Acta* 183(1):305–310

4. Yang Z, Qi C, Zheng X, Zheng J (2016) Sensing hydrogen peroxide with a glassy carbon electrode modified with silver nanoparticles, AlOOH and reduced graphene oxide. *Microchim Acta* 183(3): 1131–1136
5. Mei L, Zhang P, Chen J, Chen D, Quan Y, Gu N, Cui R (2016) Non-enzymatic sensing of glucose and hydrogen peroxide using a glassy carbon electrode modified with a nanocomposite consisting of nanoporous copper, carbon black and nafion. *Microchim Acta* 183(4):1359–1365
6. Wu Q, Sheng Q, Zheng J (2016) Nonenzymatic amperometric sensing of hydrogen peroxide using a glassy carbon electrode modified with a sandwich-structured nanocomposite consisting of silver nanoparticles,  $\text{Co}_3\text{O}_4$  and reduced graphene oxide. *Microchim Acta* 183(6):1943–1951
7. Baghayeri M, Zare EN, Lakouraj MM (2015) Monitoring of hydrogen peroxide using a glassy carbon electrode modified with hemoglobin and a polypyrrole-based nanocomposite. *Microchim Acta* 182(3–4):771–779
8. Lin Y, Chen X, Lin Y, Zhou Q, Tang D (2015) Non-enzymatic sensing of hydrogen peroxide using a glassy carbon electrode modified with a nanocomposite made from carbon nanotubes and molybdenum disulfide. *Microchim Acta* 182(9–10):1803–1809
9. Shi L, Niu X, Liu T, Zhao H, Lan M (2015) Electrocatalytic sensing of hydrogen peroxide using a screen printed carbon electrode modified with nitrogen-doped graphene nanoribbons. *Microchim Acta* 182(15–16):2485–2493
10. Yang J, Lin M, Cho M, Lee Y (2015) Determination of hydrogen peroxide using a Prussian blue modified macroporous gold electrode. *Microchim Acta* 182(5–6):1089–1094
11. Ricci F, Palleschi G (2005) Sensor and biosensor preparation, optimisation and applications of Prussian blue modified electrodes. *Biosens Bioelectron* 21(3):389–407
12. Mokrushina AV, Heim M, Karyakina EE, Kuhn A, Karyakin AA (2013) Enhanced hydrogen peroxide sensing based on Prussian blue modified macroporous microelectrodes. *Electrochem Commun* 29:78–80
13. Kong B, Selomulya C, Zheng G, Zhao D (2015) New faces of porous Prussian blue: interfacial assembly of integrated heterostructures for sensing applications. *Chem Soc Rev* 44(22):7997–8018
14. Zanfognini B, Zanardi C, Terzi F, Ääritalo T, Viinikanoja A, Lukkari J, Seeber R (2011) Layer-by-layer deposition of a polythiophene/Au nanoparticles multilayer with effective electrochemical properties. *J Solid State Electr* 15(11–12):2395–2400
15. Sau TK, Rogach AL, Jäckel F, Klar TA, Feldmann J (2010) Properties and applications of colloidal nonspherical noble metal nanoparticles. *Adv Mater* 22(16):1805–1825
16. Homok V, Dékány I (2007) Synthesis and stabilization of Prussian blue nanoparticles and application for sensors. *Interf Sci* 309(1): 176–182
17. Fiorito PA, Gonçalves VR, Ponzio EA, de Torresi SIC (2005) Synthesis, characterization and immobilization of Prussian blue nanoparticles. A potential tool for biosensing devices. *Chem Commun* 3:366–368
18. Haghghi B, Hamidi H, Gorton L (2010) Electrochemical behavior and application of Prussian blue nanoparticle modified graphite electrode. *Sensors Actuators B Chem* 147(1):270–276
19. Li N, He B, Xu S, Yuan J, Miao J, Niu L, Song J (2012) In situ formation and growth of Prussian blue nanoparticles anchored to multiwalled carbon nanotubes with poly (4-vinylpyridine) linker by layer-by-layer assembly. *Mater Chem Phys* 133(2):726–734
20. Lange U, Roznyatovskaya NV, Mirsky VM (2008) Conducting polymers in chemical sensors and arrays. *Anal Chim Acta* 614(1): 1–26
21. Bhandari S, Deepa M, Srivastava AK, Joshi AG, Kant R (2009) Poly (3, 4-ethylenedioxythiophene)-multiwalled carbon nanotube composite films: structure-directed amplified electrochromic response and improved redox activity. *J Phys Chem B* 113(28): 9416–9428
22. Sundari PA, Manisankar P (2011) Development of ultrasensitive surfactants doped poly (3, 4-ethylenedioxythiophene)/multiwalled carbon nanotube sensor for the detection of pyrethroids and an organochlorine pesticide. *J Appl Electrochem* 41(1):29–37
23. Emst A, Makowski O, Kowalewska B, Miecznikowski K, Kulesza PJ (2007) Hybrid bioelectrocatalyst for hydrogen peroxide reduction: immobilization of enzyme within organic-inorganic film of structured Prussian blue and PEDOT. *Bioelectrochemistry* 71(1): 23–28
24. Zhang Q, Zhang L, Li J (2007) “Green” synthesis of size controllable Prussian blue nanoparticles stabilized by soluble starch. *Nanotechnol* 7(12):4557–4561
25. Cao L, Liu Y, Zhang B, Lu L (2010) In situ controllable growth of Prussian blue nanocubes on reduced graphene oxide: facile synthesis and their application as enhanced nanoelectrocatalyst for  $\text{H}_2\text{O}_2$  reduction. *ACS Appl Mater Interfaces* 2(8):2339–2346
26. Xu M, Luo X, Davis JJ (2013) The label free picomolar detection of insulin in blood serum. *Biosens Bioelectron* 39(1):21–25
27. Karyakin AA (2001) Prussian blue and its analogues: electrochemistry and analytical applications. *Electroanalysis* 13(10):813–819
28. Zhang Y, Sun X, Zhu L, Shen H, Jia N (2011) Electrochemical sensing based on graphene oxide/Prussian blue hybrid film modified electrode. *Electrochim Acta* 56:1239–1245
29. Ghaderi S, Mehrgardi MA (2014) Prussian blue-modified nanoporous gold film electrode for amperometric determination of hydrogen peroxide. *Bioelectrochemistry* 98:64–69
30. Zhang Y, Luo H, Li N (2011) Hydrogen peroxide sensor based on Prussian blue electrodeposited on (3-mercaptopropyl)-trimethoxysilane polymer-modified gold electrode. *Bioprocess Biosyst Eng* 34:215–221
31. Gong H, Sun M, Fan R (2013) Qian L (2013) one-step preparation of a composite consisting of graphene oxide, Prussian blue and chitosan for electrochemical sensing of hydrogen peroxide. *Microchim Acta* 180:295–301
32. Li Y, Liu X, Zeng X, Liu Y, Liu X, Wei W, Luo S (2009) Nonenzymatic hydrogen peroxide sensor based on a Prussian blue-modified carbon ionic liquid electrode. *Microchim Acta* 165: 393–398
33. Saha BK, Ali MY, Chakraborty M, Islam Z, Hira AK (2003) Study on the preservation of raw milk with hydrogen peroxide ( $\text{H}_2\text{O}_2$ ) for rural dairy farmers. *Pak J Nutr* 2:36–42